Repository Istituzionale dei Prodotti della Ricerca del Politecnico di Bari

Quantitative analysis of QSI and LVI damage in GFRP unidirectional composite laminates by a new ultrasonic approach

This is a post print of the following article

Original Citation:
Quantitative analysis of QSI and LVI damage in GFRP unidirectional composite laminates by a new ultrasonic approach / Castellano, Anna; Fraddosio, Aguinaldo; Piccioni, Mario Daniele. - In: COMPOSITES. PART B, ENGINEERING. - ISSN 1359-8368. - STAMPA. - 151:(2018), pp. 106-117. [10.1016/j.compositesb.2018.06.003]

Availability:
This version is available at http://hdl.handle.net/11589/155917 since: 2021-03-06

Published version
DOI:10.1016/j.compositesb.2018.06.003

Publisher:

Terms of use:

(Article begins on next page)

12 October 2024

Quantitative analysis of QSI and LVI damage in GFRP unidirectional composite laminates by a new ultrasonic approach

Anna Castellano[a,*], Aguinaldo Fraddosio[b], Mario Daniele Piccioni[b]

[a]*Department of Mechanics, Mathematics and Management, Polytechnic University of Bari, Bari, Italy*

[b]*Department of Civil Engineering Sciences and Architecture, Polytechnic University of Bari, Bari, Italy*

E-mail address:

[a,*]*anna.castellano@poliba.it*, [b]*aguinaldo.fraddosio@poliba.it*, [b]*mariodaniele.piccioni@poliba.it*

Abstract

Our work is focused on a new experimental approach for the comparison between Quasi Static Indentation (QSI) damage and Low-Velocity Impact (LVI) damage in polymer composites starting from the results of ultrasonic goniometric immersion tests. In particular, the comparison is performed through the analysis of the additional anisotropy induced by the damage in unidirectional Glass Fiber-Reinforced Polymer (GFRP) composites due to QSI and LVI damage tests performed with a low level of the employed energy. To this aim, we ultrasonically reconstruct the acoustic curves (velocity curves and slowness curves) before and after the damage. Ultrasonic experiments are performed by using a goniometric ultrasonic immersion device designed and built at our laboratory, aimed at the mechanical characterization of anisotropic materials. We highlight differences and similarities between QSI and LVI damage starting from the analysis of the variations of the acoustic behavior and by using a suitable anisotropic damage model developed in the framework of the Continuum Damage Mechanics theory. The proposed experimental approach can be suitably developed for in situ investigations on low-velocity impact damage in polymer composite components.

Keywords:

A. *Low Velocity Impact test*
B. *Quasi Static Indentation test*
C. *Damage induced anisotropy*
D. *Continuum Damage Mechanics*
E. *Ultrasonic waves propagation*

F. Glass fiber reinforced composites

1. Introduction

Structural components made of fiber-reinforced polymer composites are increasingly used in several engineering applications because of their high weight-specific mechanical properties. In particular, nowadays fibre-reinforced polymer composite laminates are commonly used for aerospace [1], automotive [2], military [3], marine [4], and construction [5,6] applications.

However, the higher strength-to-weight ratio of laminated composites is counterbalanced by a significant vulnerability to impact damage, due to the absence of reinforcement through the thickness and to material discontinuities at the ply interfaces. This can considerably affect the mechanical performances of the composite, and may evolve often in unpredictable ways, leading to an unexpected and sudden failure of the structural component.

In particular, for many applications the major concern regards the damage induced by low velocity impacts (LVI). LVI are likely to occur during the various stages of the life of many components, starting from the manufacturing, keeps going during the service life and the maintenance. A typical damage process originated by a LVI may lead to the development of microcracks, fiber crushing and delamination, localized in limited area. When the structural component becomes subject to subsequent loads, related to its service life, a propagation and an evolution of the original damage can occur. This evolution of the damage can totally jeopardize the mechanical properties of the component.

It is important to recall that LVI damage may be sneaky, since after the impact often it is not possible to see any visible external sign of damage, although a significant internal degradation has taken place; in addition, the internal damage may spread over a wide area surrounding the impact point, leading to a considerable lowering of the mechanical properties of the composite.

For the above reasons, the study of LVI damage has become a key subject in the research on composites since the 1970s. Indeed, it is possible to find a broad literature about experimental analyses on the effects of LVI on composites. Several conditioning aspects have been analyzed like, e.g., the shape of the impactor, the number of impacts, the boundary conditions, the thickness of the composite, the velocity and the impact energy [7]. Moreover, the literature indicates that the results are strictly related to the composite type; by narrowing the landscape to fibre-reinforced polymer composite laminates, the effects of LVI damage depend on the content of the fibers and the matrix and on the arrangement of the layers [4,8–11].

A significant fact to underline is that LVI damage tests are relatively difficult and expensive to perform, and their results are often largely scattered and of complex interpretation. Thus, a large number of studies concern the possibility of assessing LVI damage behavior of composites starting from the results of quasi-static indentation (QSI) tests [9,12–14].

Indeed, for composite laminates the damage configuration due to quasi-static indentation is similar to that of low velocity impact [9]. Of course, the latter is a dynamic process, whereas QSI tests are performed at such a low speed that dynamical effects are negligible. This justify the simplicity and reliability in obtaining the required results from the easily controlled QSI tests; moreover, as well as in LVI tests it is possible to consider different impact energy, in QSI tests it is possible to vary the maximum achieved displacement, in order to investigate the progression of the damage.

In the literature, a number of studies indicates that the low-velocity impact and quasi-static indentation cause a similar response of composite laminates in terms of the induced damage and the residual strength. Anyway, the rate-dependency of the mechanical response of many composites may affect the representativity of the results of QSI tests in terms of the characterization of the low-velocity impact damage behavior [2].

Mostly, the results of QSI tests are compared to those obtained by LVI tests in terms of the comparison of the acquired force-displacement responses and in terms of the damage observed in the two different experimental procedures. For the latter, both destructive tests like microstructural analyses by SEM and compression after-impact tests or non-destructive tests like, e.g., ultrasonic C-scan tests and X-rays tests are performed. The aim is basically that of determining the extension of the damaged area and the features of the occurred damage.

In general, these analyses provide an understanding of the general damage resistance response, but cannot identify the process of the development of the damage, and if there are similarities in the interaction of different damage modes. Anyway, comparison of QSI damage and LVI are performed for the same employed energy [15].

On the other hand, since LVI damage is considered very difficult to detect, there is also a broad literature about non-destructive techniques for detecting, quantifying and monitoring LVI damage on composite laminates. Among the others, ultrasonic [1,15], ultrasonic guided waves [16], thermographic [17,18], holographic [19] and acoustic emission techniques have been studied.

Here, we propose a new approach for the comparison between the damage induced by LVI tests and QSI tests in glass fiber-reinforced polymer composites (GFRP). We consider the damage resulting from low impact energy, in view of representing possible scenario where the impact generates sneaky damages, difficult to detect, but capable of evolving in a sudden failure of the composite.

Since the damage of composites involves a damage induced anisotropy superimposed to the constitutive anisotropy [20–22], our approach is based on the employ of ultrasonic goniometric tests, based on the analysis of change in the anisotropy of the acoustic response of the composites.

Goniometric ultrasonic tests combined with ultrasonic immersion techniques and ultrasonic laser techniques have been proven to be effective tools for the characterization of the mechanical response of anisotropic materials [23,24] since it is possible to access to all the elastic constants in a relatively easy way. Here the task is a little bit more complicated, since we have to experimentally distinguish the damage induced anisotropy from the original constitutive anisotropy of the material. To this aim, we employ an innovative goniometric ultrasonic immersion device designed and built at our laboratory [25].

The study of the damage is based on the analyses of the changes in the velocity curves and in the slowness curves before and after the damage. Moreover, a quantitative evaluation of the damage is provided by employing an anisotropic damage model developed within the Continuum Damage Mechanics (CDM) [26,27], and based on a tensorial damage measure. For determining the components of this damage measure, the change of the elastic constants due to the damage is evaluated.

By comparing the characteristic acoustic curves of QSI and LVI damaged GFRP composites and by using the above cited damage measure, we discuss similarities and differences between the acoustic features of the damage induced by the two different damage tests, and the differences in the macroscopic characterization of the occurred damage.

Moreover, since the experimental approach here presented can be further developed for in-situ applications, this study can be useful for linking the damage level detected on in-service structural components to the results of laboratory analysis on LVI damage performed on composite laminates.

Indeed, the present work takes inspiration from the research activities carried out for answering the needs of damage characterization and evaluation of composites arisen in a research project on the development of on innovative wind turbine blades, molded in only one piece, and made of unidirectional GFRP laminate (Fig. 1).

Wind turbine blades are very sensitive to damage, and in particular to low-velocity impact damage, for impacts that can occur during the manufacturing, the transportation and the installation, or during the service life owing to foreign objects, heavy hailstones, etc.. Thus it is crucial not only an accurate structural design against the damage induced by possible impacts expected during the service life, but also to develop quantitative approaches for in-situ damage characterization.

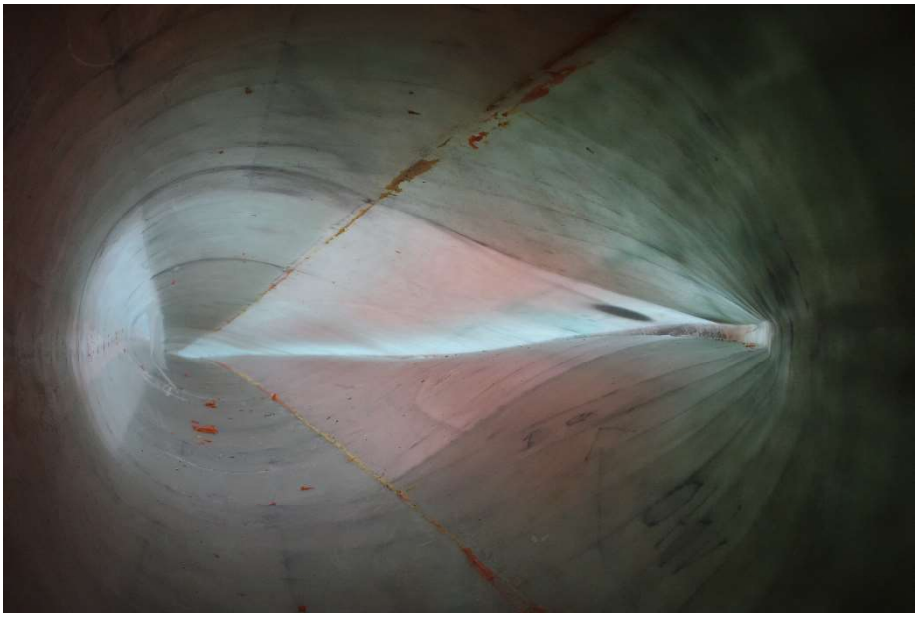

Fig. 1. Inner view of an innovative GFRP wind turbine blade entirely molded in only one piece

The paper is arranged as follows. In Sect. 2 we briefly summarize the theoretical framework. First, (Sect. 2.1) we set the analysis of wave propagation in anisotropic solids in the framework of the linear electrodynamic theory; we then specialize the topic to the special case of transversely isotropic materials. Then, (Sect. 2.1) we recall the fundamentals on damage models for anisotropic solids, and we present more in depth an effective anisotropic damage models for the interpretation of the results of ultrasonic experiments on damaged composites.

Sect. 3 is devoted to the experimental procedure. After a general presentation (Sect. 3.1), we describe the experimental setup employed for performing ultrasonic goniometric immersion tests, the examined samples, and the interpretation of the results of the tests in terms of the classification of the anionotropy degree of the material and of the determination of the independent elastic constants needed for the description of the elastic behavior of the composite (Sect. 3.2). Finally, in Sect. 3.3 we introduce the performed LVI and QSI damage tests.

The obtained results are discussed in Sect. 4; this discussion is aimed not only at the characterization of the damage, but also at the comparison of the identified similarities and differences between LVI and QSI damage. First (Sect. 4.1) we show the ultrasonic velocity curves and the ultrasonic slowness curves, both for the undamaged composites and for QSI damaged and LVI damaged composites. In Sect. 4.2 the estimated elastic constants both for the undamaged samples and for QSI damaged and LVI damaged samples are presented; moreover, the variation of the elastic constants due to the damage is discussed. Finally, in Sect. 4.3 we show the values obtained for the components of the tensorial damage measure both for QSI damaged and LVI damaged composites.

2. Theoretical framework

2.1 The linear elastodynamic theory

Wave phenomena involved in ultrasonic experimental tests are usually described by the linearized elastodynamic theory. Indeed, ultrasonic waves of small energy, like those employed for the experiments, can be regarded as small perturbations of a reference (eventually prestressed [28,29]) state of an elastic body.

Here, we study the case of solid bodies in a stress-free reference configuration, so that we may refer to the simpler framework of the linear elastodynamic theory [30]. In particular, we search solutions in the form of progressive plane waves for the equation of motion

$$\mathrm{Div}\left(\mathbb{C}\left[\nabla\mathbf{u}\right]\right) = \rho\ddot{\mathbf{u}}, \tag{1}$$

where $\rho=\rho(\mathbf{x})$ is the mass density, $\mathbb{C}=\mathbb{C}\left(\mathbf{x}\right)$ is the fourth order elasticity tensor endowed with the first and the second minor symmetries [30], $\mathbf{u}=\mathbf{u}(\mathbf{x})$ has the following form:

$$\mathbf{u}\left(\mathbf{x},\mathrm{t}\right) = \mathbf{a}\ \varphi\left(\mathbf{x}\cdot\mathbf{n} - \mathrm{v}\,\mathrm{t}\right) \tag{2}$$

and represents a progressive elastic plane wave with propagation direction **n**, direction of motion **a**, propagation velocity v; finally, φ is a real valued smooth function.

The propagation of plane progressive elastic waves in an elastic body is ruled by the Fresnel-Hadamard condition [30]:

$$\left[\mathbf{\Gamma}\left(\mathbf{n}\right) - \rho\mathrm{v}^2\mathbf{I}\right]\mathbf{a} = \mathbf{o}, \tag{3}$$

where $\mathbf{\Gamma}\left(\mathbf{n}\right)$ is the second order Kelvin-Christoffel propagation tensor for the direction **n**, related to the elastic tensor $\mathbb{C}$ as follows:

$$\mathbf{\Gamma}\left(\mathbf{n}\right) = \mathbb{C}^{\mathrm{t}}\left[\mathbf{n}\ \otimes\ \mathbf{n}\right] \tag{4}$$

(in (4), the superscript "t" represents the minor transposition for fourth order tensors).

By (3)-(4), if an elastic wave propagates in a given direction **n**, the square of the propagation velocity v is an eigenvalue of the Christoffel tensor $\mathbf{\Gamma}(\mathbf{n})$ while the direction of motion **a** is the associated eigenvector. It is clear that the symmetry properties of the elastic tensor $\mathbb{C}$ strongly influence the features of progressive elastic waves propagating along a certain direction **n**. Moreover, once fixed the propagation direction **n**, according to the polarization vector **a** *pure* propagation modes like longitudinal waves (**a** and **n** parallel) and transverse waves (**a** and **n** perpendicular), or *not pure* propagation modes (neither longitudinal or transverse waves), are possible into an elastic body. *Not pure* modes are usually classified in the literature as *quasi-longitudinal* waves or as *quasi-shear* waves, depending on the proximity of the direction of **a** to the direction of **n** or to a direction orthogonal to **n**. *Not pure* modes characterize the acoustic behaviour of anisotropic materials like composites materials; for more details, refer to [25,30,31].

This theoretical framework suggests a non-destructive ultrasonic experimental counterpart: indeed, the results of ultrasonic tests can be employed for facing two major problems in the mechanics of elastic materials: 1) the *classification problem*, that is the determination of the symmetry class and the identification of the material symmetry axes; 2) the *representation problem*, that is, once known the symmetry class, the determination of the components of the elastic tensor $\mathbb{C}$ characterizing the elastic response of the material [25].

Starting from experimental measures of ultrasonic waves velocities propagating in different directions and having different polarizations, it is possible to reconstruct three characteristic families of acoustic surfaces for the elastic materials: the *velocity surfaces,* the *wavefront surfaces* and the *slowness surfaces* [31]. In particular, a slowness surface is the polar diagram of the inverse of the phase velocity v as a function of the direction of propagation **n** of acoustic waves having a certain polarization. By considering the three possible polarizations, a family of three sheet of slowness surfaces is obtained. Each of these surfaces can be considered as generated by the variation with the direction of propagation **n** of the *slowness vector* **s**, given by the ratio between the wave number vector **k** and the angular frequency ω [31].

In case of wave propagation into isotropic elastic bodies, only pure modes are possible and the slowness surfaces consist of three pure wave sheets. Moreover, since wave velocities do not depend on the direction of propagation **n**, each slowness surface consists in a sphere whose radius is the inverse of the phase velocity: indeed, phase and group velocity vectors are collinear. Instead, in case of acoustic waves in anisotropic elastic bodies, phase velocity and group velocity vectors are no longer collinear, and then the shape of the slowness surfaces is no longer spherical. Indeed, depending

on the anisotropy features of the material, the shape of the slowness surfaces may be very complex. The experimental reconstruction of the slowness surfaces allows for identifying the material symmetry axes, also called the acoustic axes of the materials in the context of wave propagation problems [31,32]: this allows for solving the *classification problem* for the examined material. We recall the following properties of waves propagating in the direction of a material symmetry/acoustic axis [33]: for each wave propagation mode, phase velocity and group velocity share the same direction; 2) according to the Federov-Stippes theorem [30], for some symmetry classes (for example, this is the case of the transverse isotropy) two shear waves orthogonally polarized have the same phase velocity.

Since the experimental tests discussed in this paper concern unidirectional fiber reinforced composites, we may assume that the elastic response of the undamaged composite can be modeled as transversely isotropic. In particular, in a reference system whose x_3-axis is coincident with the transverse isotropy axis (that is, the x_3-axis is parallel to the fibers direction of the composite), the elasticity tensor $\mathbb{C}$ has the following representation in Voigt notation

$$\mathbb{C} = \begin{bmatrix} C_{11} & C_{12} & C_{13} & 0 & 0 & 0 \\ C_{12} & C_{11} & C_{13} & 0 & 0 & 0 \\ C_{13} & C_{13} & C_{33} & 0 & 0 & 0 \\ 0 & 0 & 0 & C_{44} & 0 & 0 \\ 0 & 0 & 0 & 0 & C_{44} & 0 \\ 0 & 0 & 0 & 0 & 0 & C_{66} \end{bmatrix}, \tag{5}$$

with $C_{12}=C_{11}-2C_{66}$.

Fig. 2 shows the theoretical slowness curves in π_{13} plane (sections of the slowness surfaces by π_{13} plane) for a transversely isotropic material; we distinguish the curves related to the differently polarized ultrasonic waves by using different colors. Notice that for a transversely isotropic elastic material having x_3-axis as the transverse isotropy axis the slowness surfaces are rotationally symmetric about x_3-axis, and have reflection symmetry about the π_{12} plane [31].

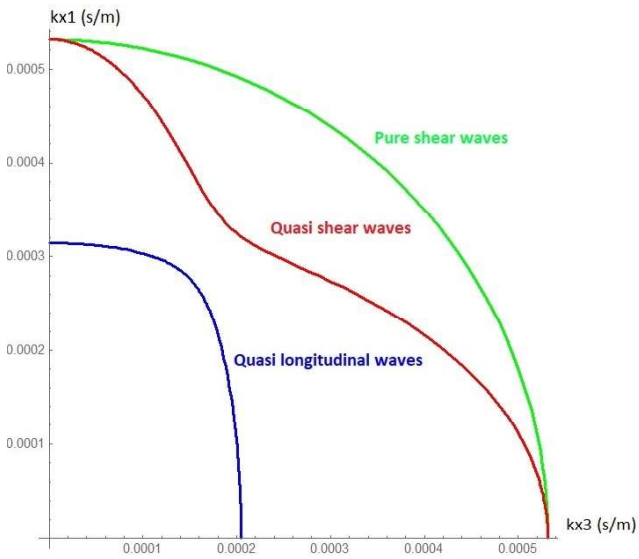

Fig. 2. Theoretical slowness curves for transversely isotropic materials with x_3-axis as the transverse isotropy axis

2.2 Anisotropic damage models for damaged composite materials

Fibre-reinforced composite materials may undergo different damage phenomena like, for example, microcracks, cavitation, decohesion at fibre ends, debonding, crazing, etc.. In general, damage is related to the deterioration of the mechanical properties of the material due to microscopic, mesoscopic and macroscopic processes: starting from the initiation of microcraks or microcavities until to the coalescence of the microscopic cracks leading, from the macroscopic point of view, to the initiation and the development of macrocracks.

Continuum Damage Mechanics (CDM) [34,35] aims at the study of the damage in materials from the mesoscopic and macroscopic point of view, in the theoretical framework of Continuum Mechanics [36]. In this framework, the damaged material is considered as a continuum, in spite of the presence of microcavities and microcracks and then, according to the principle of local state [37,38] a damage state is described at the macroscopic scale in terms of suitably damage internal variables, which represent the irreversible changes occurring at the microscopic level. By using the notion of the effective stress [39,40] and by making the assumption of the mechanical equivalence between the damaged material and a "fictitious" undamaged material, arising from the hypothesis of the strain (stress) equivalence [41,42] or from the hypothesis of the stress-energy (strain-energy) equivalence [35,42,43], CDM theoretical models provide systematic methods to formulate the constitutive equations of damaged materials.

Since the development of microcracks induces a reduction of the stiffness, the damage can be efficiently associated to the variation in elastic moduli [35,42]. Various damage models have been

formulated in the literature, taking into account different kind of damage internal variables: scalar, vectorial and tensorial internal variables (second order, fourth order and eighth order damage tensorial internal variables) [44].

Since composites are constitutively anisotropic materials and since the damage, in general, involves an anisotropization of the mechanical response (damage induced anisotropy), from an ultrasonic point of view the damage may be related to a damage induced anisotropy superimposed to the initial anisotropy of the undamaged material.

Here, starting from the results of ultrasonic tests, we study the low velocity impact (LVI) damage for glass fiber reinforced composites. In particular, we compare the damage caused by a LVI test with the damage induced by an equivalent quasi static indentation (QSI) test. For a quantitative evaluation of the damage, we ultrasonically characterize a CDM model proposed by Baste and Audoin [26,27] and aimed at the interpretation of the results of ultrasonic tests on damaged anisotropic materials; this model is based on a fourth order tensorial damage measure.

First we observe that by referring to Voigt notation, it is possible to employ the following symmetric tensor for describing the absolute variation of the elastic tensor components (stiffness)

$$\omega_{ij} = C_{ij} - \tilde{C}_{ij}, \quad i,j=1,...,6, \tag{6}$$

where the wavy stiffness refer to the damaged material, while the unmarked stiffness refer to the undamaged material.

In phenomenological damage models based on the thermodynamics of the internal variables, the damage variables vary from zero (undamaged material) to 1 (damaged material). The easier way for representing the damage for anisotropic materials is given by the tensor collecting the relative stiffness variations, that is, in Voigt notation:

$$\hat{D}_{ij} = 1 - \frac{\tilde{C}_{ij}}{C_{ij}}, \quad i,j=1,...,6. \tag{7}$$

The definition (7) involve some theoretical inconsistencies for the off-diagonal components of the damage tensor. Indeed, in order to have that all the components of the damage tensor vary in the interval [0,1], it is necessary to normalize the damage components by their thermodynamically admissible maximum values, coming from the requirement that the elasticity tensor of the damaged material is still a positive defined tensor.

According to [26] , when the stiffness of the damaged material becomes zero we obtain from (6) the maximum admissible values for the damage diagonal components ω_{ii}^{lim}; those maximum admissible values correspond to the failure of the volume element in the direction i (i=1,2,3), and in the shear plane 2,3 (i=4) or 1,3 (i=5) or 1,2 (i=6) [45], respectively

$$\omega_{ii}^{lim} = C_{ii} > 0 \ , \quad i=1,...,6 \ . \tag{8}$$

Instead, for off-diagonal damage components the admissible maximum values ω_{ij}^{lim} correspond to the fact that a minor $M_{ij} = \tilde{C}_{ii}\tilde{C}_{jj} - \tilde{C}_{ij}^{2}$ of the damaged elastic tensor becomes equal to zero. Hence, we have:

$$\omega_{ij}^{lim} = C_{ij} \pm \sqrt{\tilde{C}_{ii}\tilde{C}_{jj}} \ , \ i,j=1,...,6, \ i \neq j. \tag{9}$$

In (9) the sign ± depends on the admissible variation of $\tilde{C}_{ij}$; in particular, we have an upper bound for $\tilde{C}_{ij}$ when $\omega_{ij} < 0$ and a lower bound for $\tilde{C}_{ij}$ when $\omega_{ij} > 0$:

$$-\sqrt{\tilde{C}_{ii}\tilde{C}_{jj}} < \tilde{C}_{ij} < \sqrt{\tilde{C}_{ii}\tilde{C}_{jj}} \ . \tag{10}$$

By the above, a thermodynamically consistent tensorial damage measure **D** for anisotropic material may be defined such that, in Voigt notation, the normalized diagonal components D_{ii} are:

$$D_{ii} = \frac{\omega_{ii}}{\omega_{ii}^{lim}} = 1 - \frac{\tilde{C}_{ii}}{C_{ii}}, \quad i=1,2,...,6, \tag{11}$$

and the normalized off-diagonal components D_{ij} are:

$$D_{ij} = \frac{\omega_{ij}}{\omega_{ij}^{lim}} = \frac{C_{ij} - \tilde{C}_{ij}}{C_{ij} + \mathrm{sign}\left(C_{ij} - \tilde{C}_{ij}\right)\sqrt{C_{ii}\left(1-D_{ii}\right)C_{jj}\left(1-D_{jj}\right)}}, \quad i, j=1,2,...,6, \quad i \neq j. \tag{12}$$

We observe that if the norm |**D**| of the damage tensor **D** is equal to 0, the material does not have damage; if 0<|**D**|<1, the material is damaged; if |**D**|=1, the material is totally damaged (failure of the material).

Moreover, in terms of **D** and of the stiffness of the undamaged material the stiffness of the damaged material may be expressed as follows:

$$\tilde{C}_{ii} = C_{ii}(1 - D_{ii}), \quad i=1,2,...,6, \tag{13}$$

$$\tilde{C}_{ij} = C_{ij}\left(1\text{-}D_{ij}\right) \mp D_{ij}^{\pm}\sqrt{C_{ii}\left(1\text{-}D_{ii}\right)C_{jj}\left(1\text{-}D_{jj}\right)}, \quad i, j=1,2,...,6, \quad i \neq j. \tag{14}$$

Notice that the considered fourth order damage tensor **D** possess full symmetry properties (minor symmetries and major symmetry); other approaches in the literature (see, e.g., Cauvin and Testa [46] and Olsen-Kettle [47]) refer to fourth order damage tensors equipped only the by the minor symmetries. Indeed, it is possible to show that if the latter properties holds, the major symmetry of the elastic tensor of the damaged material is ensured.

3. Experimental tests

3.1 A new experimental approach for the comparison between QSI damage with LVI damage by using ultrasonic immersion tests

We have developed an experimental procedure for the comparison between the damage induced by QSI tests and LVI tests, respectively, based on a ultrasonic immersion technique. In order to achieve this goal, we have employed an innovative ultrasonic immersion goniometric device designed and built by our laboratory (Laboratorio "M. Salvati") [24,25]. This device allows for rotating a composite sample immersed into a water tank also housing the ultrasonic probes. As the angle of incidence between the ultrasonic beam and the sample surface varies, the Snell law show that it is possible to propagate any kind of polarized ultrasonic waves into the sample, both *pure* (longitudinal and shear waves) and *not pure* waves (quasi-longitudinal and quasi-shear waves). This way, starting from the ultrasonic results, it is possible to determine the material symmetry axes or acoustic axes (*classification problem*) and the components of the elastic tensor (*representation problem*).

Ultrasonic tests have been performed on two composite samples before and after a LVI test and a QSI test, respectively. The main steps of the procedure are following:

1) Evaluation of the velocity of ultrasonic waves with different polarizations and different propagation directions for the undamaged and for the damaged composites, for each propagation plane experimentally accessible.
2) *Classification* of the symmetry of the mechanical response of the undamaged and damaged composites by the experimental reconstruction of ultrasonic wave velocities curves and slowness curves.
3) *Representation* of the mechanical response of the undamaged and damaged composites by the determination of the required independent components of the elastic tensor.
4) Qualitative analysis of the damage induced anisotropy for the examined composites through the comparison between ultrasonic wave velocities curves and slowness curves of the undamaged and damaged (QSI damaged and LVI damaged, respectively) composites.
5) Quantitative analysis of the damage induced anisotropy for the examined composites by: a) the comparison between the elastic constants evaluated for the undamaged and damaged (QSI damaged and LVI damaged, respectively) composites; b) the determination of the components of damage tensor (11)-(12) in case of QSI damage and LVI damage, respectively, which definitively allows for a quantitative and synthetic evaluation of the occurred damage.

In Sect. 4 we show the main results achieved by the procedure described above.

3.2 Ultrasonic goniometric immersion tests

Ultrasonic tests were performed by using an innovative goniometric immersion device specifically designed for the mechanical characterization of anisotropic materials like composites [24,25]. The device consists in: an immersion water tank; a frame housing ultrasonic immersion transducers and/or a reflective surface in Plexiglas; a rotating slot for the sample operated by a stepper motor with a reducer gearbox characterized by a very small angular steps (0.036°) (Fig. 3). This device can be used in two different configurations: through-transmission tests and back-reflection tests. For the present study, we used the latter configuration: ultrasonic waves are generated and received by an unfocused ultrasonic immersion probe with a central frequency of 1 MHz. The ultrasonic signals are handled by an ultrasonic pulser/receiver Olympus 5072PR and an oscilloscope Agilent DSO6014A (100 MHz, 4 channels).

The controller of the motor stepper and the analysis and the processing of ultrasonic signals are managed by a LabVIEW software ad hoc designed for performing the ultrasonic goniometric immersion tests. For each rotation angle of the sample, by this software the time of flight (TOF) Δt of ultrasonic waves is determined through the cross-correlation between the auto-correlated reference signal (ultrasonic signals acquired without sample) and the average of the normalized signals acquired

(ultrasonic signals acquired with the sample placed in the slot) [25]. At the end of each ultrasonic test, the LabVIEW software displays a graph showing the measured ultrasonic phase velocities v_p (m/s) versus the angle of incidence θ (deg) of the ultrasound beam (Fig. 4).

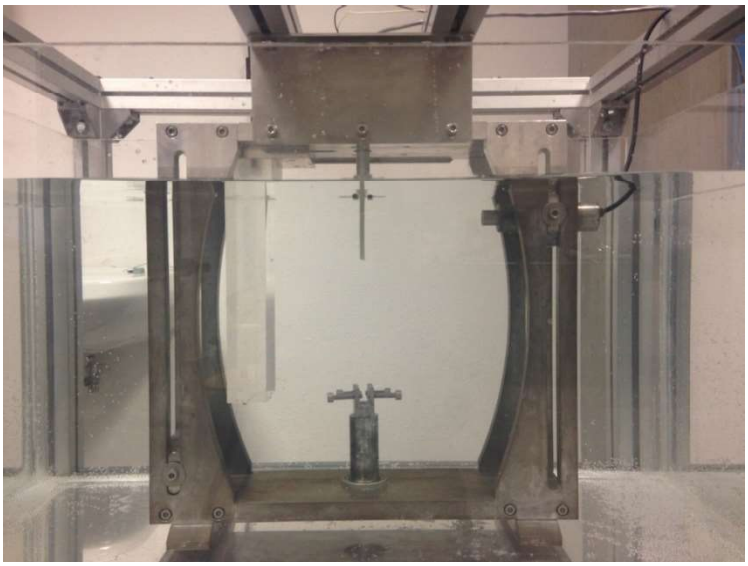

Fig. 3. Goniometric ultrasonic immersion device

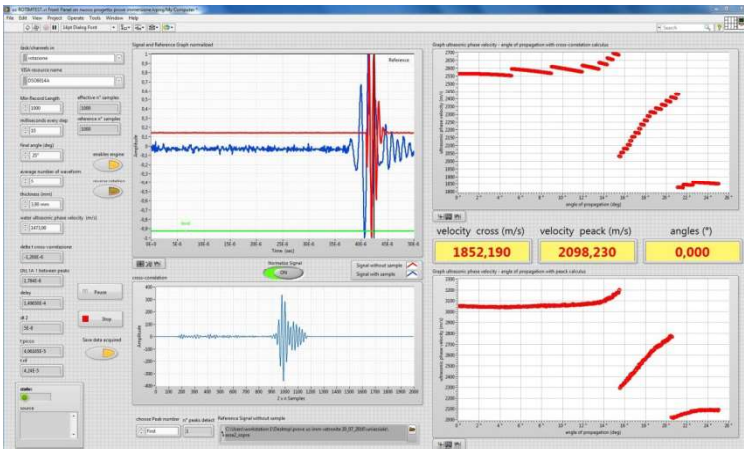

Fig. 4. LabVIEW software interface

We employed the above described device for ultrasonically characterizing the mechanical response of glass fiber–reinforced composites made of 4 unidirectional fiberglass reinforced layers with an overall thickness of 3.8 mm used for the construction of innovative wind turbine blades, as mentioned in the Introduction.

In particular, we have ultrasonically characterized the mechanical behaviour of two glass fiber reinforced composite samples: one indicated as S1 and another as S2 (Fig. 5). For both samples we have first performed the ultrasonic tests on the undamaged material. Then, S1 sample has been

damaged by a quasi-static indentation (QSI) test, whereas S2 sample has been damaged by a low-velocity impact (LVI) test. Finally, ultrasonic tests have been performed again on the two damaged samples.

Fig. 5. Undamaged GFRP composite samples S1 and S2

As discussed in Sect. 2.1, we have initially assumed that the mechanical response of the undamaged unidirectional composite can be described as transversely isotropic linearly elastic. By the experimental reconstruction of ultrasonic wave slowness curves, it was possible to confirm this initial hypothesis, since those curves are practically superimposed to the corresponding theoretical curves. In this way, we have ultrasonically solved the *classification problem*.

Then, once determined the mass density ρ of the composite samples, the phase velocity data recorded by the LabViEW software allowed us to determine by the inversion of the Christoffel equation (3) the independent elastic constants of the composites (*representation problem*). In our case, we determined the five elastic independent constants (C_{11}, C_{13}, C_{33}, C_{44} and C_{66}) needed for the description of the linear elastic behavior of a transversely isotropic material. To this aim, we have considered two different propagation planes: the plane $\pi_{12,}$ which allowed us to measure C_{11}, C_{44} and C_{66}, and the plane π_{13} (the plane containing the fibres), enabled us for the measurement also of C_{33} and C_{13} (Fig. 6).

For inducing wave propagation in the plane π_{12}, we placed the samples in the ultrasonic device so that the rotation axis of the sample was parallel to x_3-axis (i.e., the fiber axis). Wave propagation in the plane π_{13} was obtained by placing the sample with the rotation axis orthogonal to the axis of the fibers, and coincident with the x_2-axis.

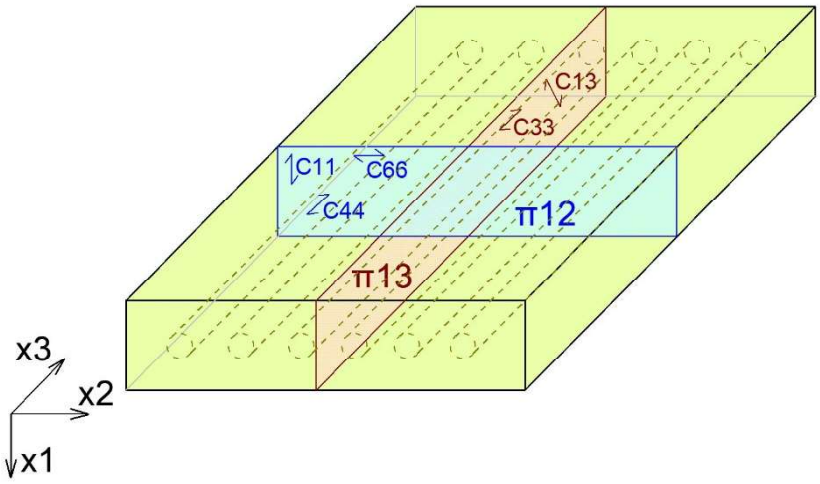

Fig. 6. Geometrical scheme of the unidirectional composite with the indication of the propagation planes and of the related elastic constants

The same procedure has been repeated on the damaged samples. In both cases (QSI damaged S1 sample and LVI damaged S2 sample), the comparison between the experimental reconstructed slowness curves and the corresponding theoretical curves allows us for considering the elastic response of the damaged materials still as linear transversely isotropic elastic. Then, by the inversion of the Christoffel equation (3), we have determined the five elastic independent constants for the QSI damaged S1 sample and for the LVI damaged S2 sample.

3.3 Damage tests: Quasi Static Indentation (QSI) test and Low Velocity Impact (LVI) test

As mentioned in Sect. 2.1, two different damage tests were conducted on the examined GFRP composite samples: a quasi-static indentation (QSI) test on the sample S1, and a low-velocity impact (LVI) test on the sample S2.

In either test, we used a hemispherical impactor acting in the x1-direction, with diameter 57 mm and weight 0.959 kg.

The QSI test was performed by using a electromechanical Instron universal testing machine and according to the ASTM D6264 [48] standard. The S1 sample was clamped at the corners and was indented by the impactor with a peak load of 344 N and peak energy level of 1.90 J.

For LVI test an in-house built impact set-up was employed, and the test was performed according to ASTM D7136 standard [49]. The S2 sample was hit by the hemi-spherical impactor with a impact velocity of 1.944 m/s; the measured impact energy level was 1.90 J.

The low value of the impact energy considered for the experiments (1.90 J) was aimed at damaging the composites without break it. According to the literature [15], since the energy level of both the performed LVI and QSI damage tests is the same, similar damage effects are expected.

Fig. 7. Damaged GFRP composite samples S1 and S2

4. Results

4.1 Ultrasonic wave velocities curves and slowness curves

We first provide a *qualitative* comparison between QSI and LVI damage through the analysis of the ultrasonic wave velocities curves obtained for the undamaged and the damaged samples, respectively. Fig. 8 shows the graphs phase velocity vs incident angle for the sample S1 before and after the QSI damage test, for wave propagation in the plane π_{12}, orthogonal to the fibers. In particular, we have plotted in green the results obtained for the undamaged composite, and in orange the results obtained for the QSI damaged composite.

According to the Snell's law, we observe a mode conversion from pure longitudinal (PL) waves to pure shear (PS) waves at the first critical angle.

We notice that the QSI damage has induced a slight reduction both of the phase velocity of PL waves and of the first critical angle (from about 10,12° to about 9,47°). For the velocity of PS waves no remarkable difference are noticeable between the undamaged sample and the damaged sample.

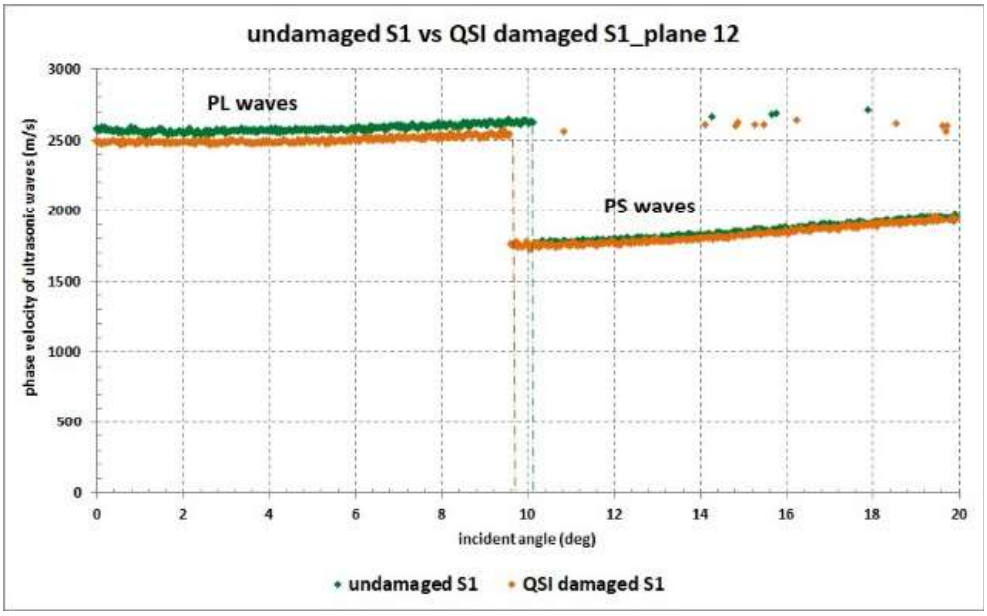

Figure 8: Ultrasonic wave velocity curves (plane π_{12}, undamaged vs QSI damaged sample S1)

In Fig. 9 we have reported the graphs phase velocity vs incident angle for the sample S2 before and after the LVI damage test, and for the propagation plane π_{12}. Here, we have plotted in blue the results obtained for the undamaged composite, and in red the results obtained for the LVI damaged composite.

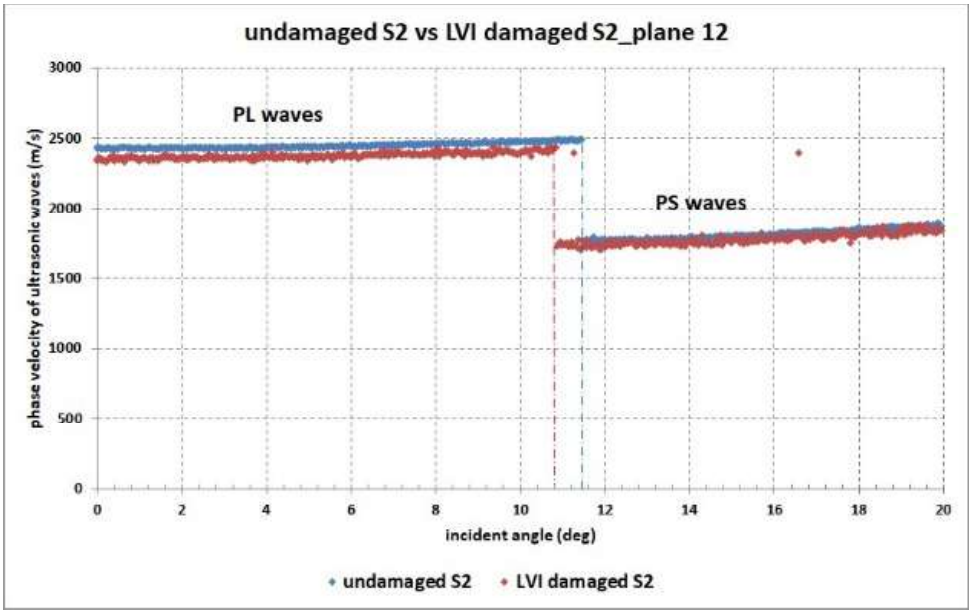

Figure 9: Ultrasonic wave velocity curves (plane π_{12}, undamaged vs LVI damaged sample S2)

Also in this case, we see that LVI damage induces a small decrement of the phase velocity of PL waves, and a slight reduction of the value of the first critical angle, from about 11,30° to about 10,69°.

After the first critical angle, PS waves are observed, but the curve related to the undamaged sample is almost overlapped to that related to the damaged sample.

For what concerns the propagation of waves in the plane π_{13}, the graphs phase velocity vs incident angle obtained for sample S1 before and after the QSI damage test and for sample S2 before and after the LVI damage test are reported in Figg. 10 and 11, respectively.

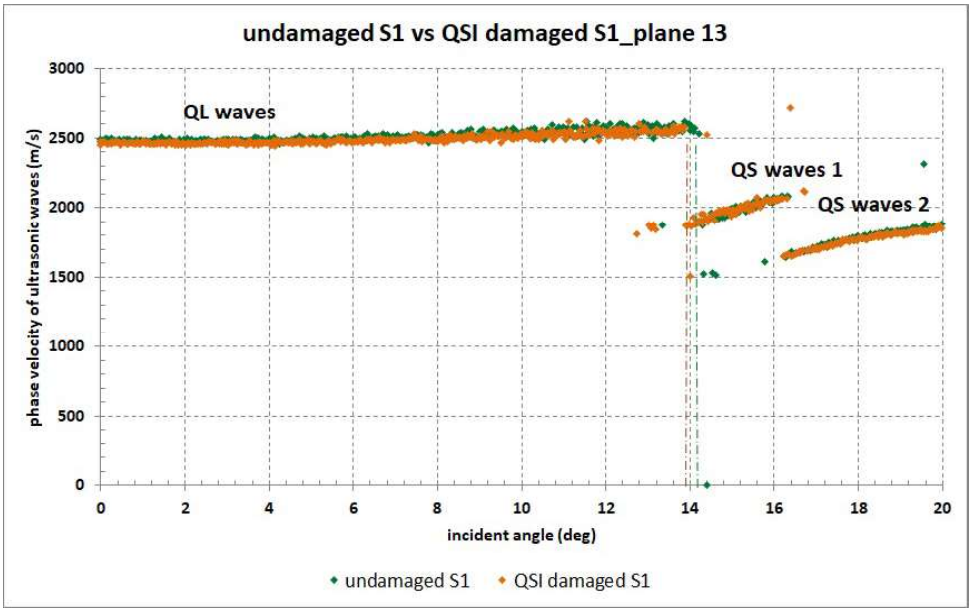

Figure 10: Ultrasonic wave velocity curves (plane π_{13}, undamaged vs QSI damaged sample S1)

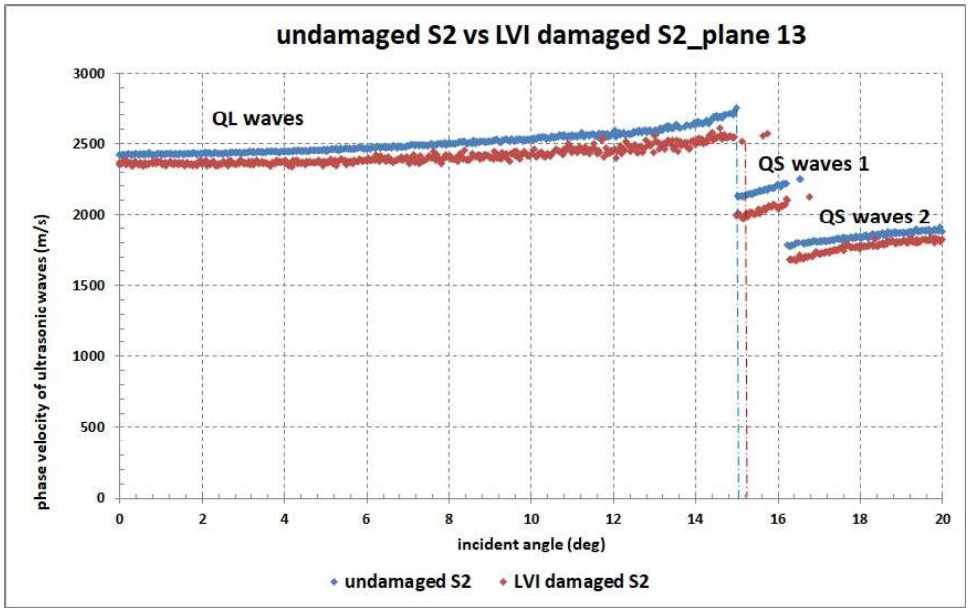

Figure 11: Ultrasonic wave velocity -curves (plane π_{13}, undamaged vs LVI damaged sample S2)

In both graphs, we observe a first mode conversion from quasi longitudinal (QL) waves to a first kind of quasi shear waves (QS waves 1), and then from the latter to a second kind of quasi shear waves (QS waves 2). The results obtained for the propagation plane π_{13} show a more marked variation of the acoustic response of the composites samples due to the damage, especially for what concerns the LVI damaged sample S2. Indeed, Fig. 11 shows that LVI damage involves a noticeable reduction of the velocity of all the three kinds of polarized waves propagating in the sample. On the other hand, see Fig. 10, the effect of QSI damage in terms of velocity reduction is discernible only for QL waves. In both cases (QSI damage and LVI damage), a reduction of the first critical angle is observed.

Starting from the experimental measured phase velocities of ultrasonic waves, we reconstructed the slowness curves for wave propagation in the plane π_{13}, for both the examined composite samples, before and after the damage.

Fig. 12 shows the experimental slowness curves for S1 sample before (a) and after the QSI damage test (b), respectively. We observe only a slight variation of the slowness curve for each kind of polarized ultrasonic waves, and this correspond to the fact that QSI test has induced a very small damage anisotropy in the composite sample S1.

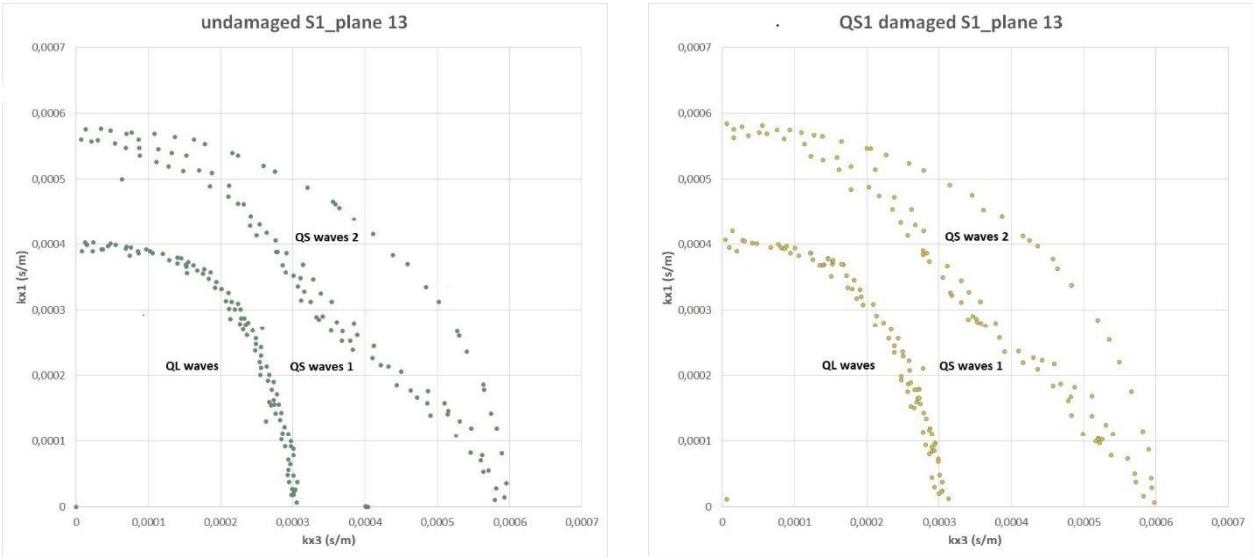

(a) (b)

Figure 12: Experimental slowness curves of undamaged and QSI damaged sample S1 (propagation in π_{13} plane)

Notice that the comparison of the shapes of these experimental slowness curves with the shapes of theoretical slowness curve in Fig. 2 confirms the hypothesis of transversely isotropic elastic response both before and after QSI damage tests. Moreover, the velocities of the two quasi shear waves propagating along x_3-axis before and after the damage are the same: this implies that the damage

induced by QSI test has not varied the acoustic axis of the composite, i.e., the transverse isotropy axis.

Fig. 13 shows the experimental slowness curves for S2 sample before (a) and after LVI damage test (b), respectively. Also in this case, the comparison of the experimental slowness curves with the theoretical ones (see Fig. 2) confirms the hypothesis of transversely isotropic elastic response, both for the undamaged and for the LVI damaged composite.

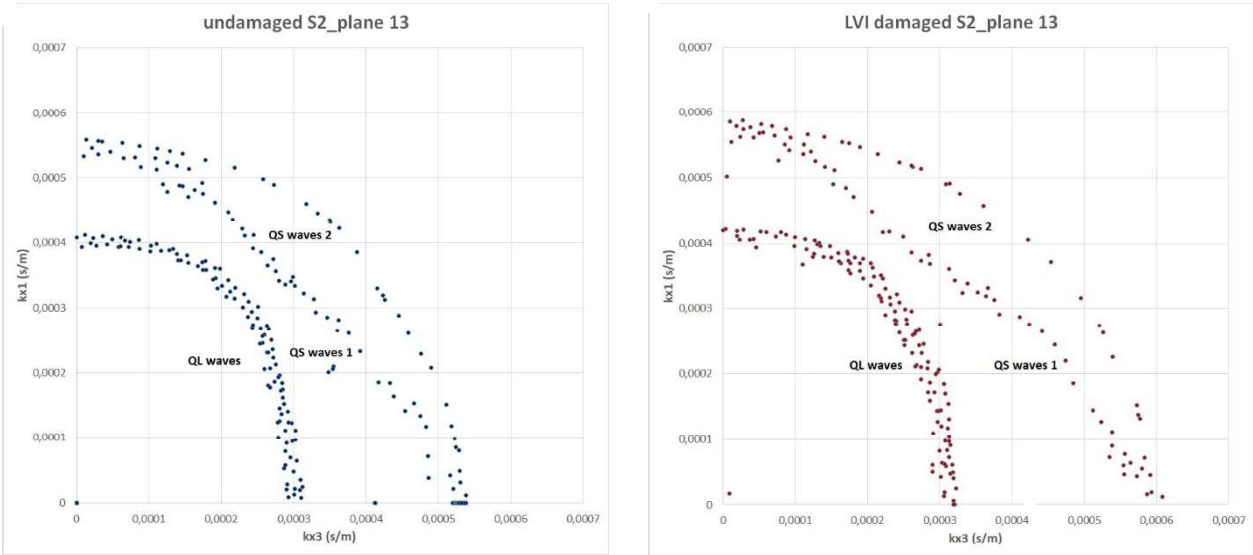

(a) (b)

Figure 13: Experimental slowness curves of undamaged and LVI damaged sample S2 (propagation in π_{13} plane)

In the case of LVI damage we observe a more marked increment of the values of slowness for ultrasonic waves in the proximity of the x_1-axis (direction of the impact) and of the x_3-axis (the transverse isotropy axis). This confirms what we have yet observed about the velocity curves: the acoustic behavior of the LVI damaged composite is different from that of the QSI damaged composite. In particular, despite of the energy equivalence of the two performed damage tests, the LVI damage test induced a increase of the material anisotropy in the directions of the two axes x_1 and x_3 greater than the additional anisotropy induced by the QSI damage test. Anyway, in both cases, the damage induced anisotropy do not vary the acoustic axis of the GFRP composite (x_3-axis).

4.2. Elastic constants

Starting from the experimental results above discussed, and once measured the density of the samples, we passed to solve the *representation problem* for the considered composites before and after the two different damage tests. To do this, the inversion of the Christoffel equation (3) is needed. Since we have a redundant set of experimental data (for each propagation direction and for each polarization,

(3) gives a non-linear equation in the elastic constants [31]), for enhancing the precision in the determination of the 5 independent elastic constants we have performed a last square regression analysis, minimizing the error between experimental and theoretical values [50].

As explained in Sect. 3.1, a first *quantitative* evaluation of the damage induced anisotropy in the examined composites can been carried out by means of the analysis of the variation of the elastic constants due to the damage.

In Fig. 14, we have represented the values of the 5 independent elastic constants of the undamaged and of the QSI damaged sample S1, respectively. We see that by comparing the elastic constants of the undamaged and of the damaged composite, the macroscopic features of the damage become more evident. In particular, for the QSI damaged S1 sample we observe:

- a reduction of about 3% to 4% of the elastic constants C_{11} and C_{33} (extensional stiffness in the directions of x_1-axis, i.e. the direction of the indentation, and of x_3-axis, i.e. the transverse isotropy axis, respectively) and of the shear elastic constant C_{44};
- a very small decrement of the shear elastic constant C_{66};
- a reduction of about 7% of the shear elastic constant C_{13}.

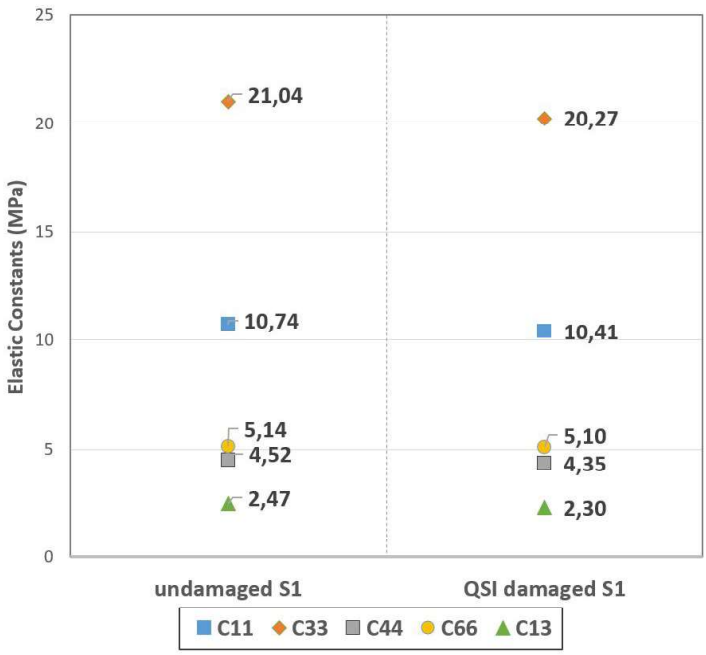

Figure 14 Elastic constants of the undamaged and QSI damaged S1sample

In Fig. 15, we have represented the values of the 5 independent elastic constants of the undamaged and of the LVI damaged sample S2, respectively.

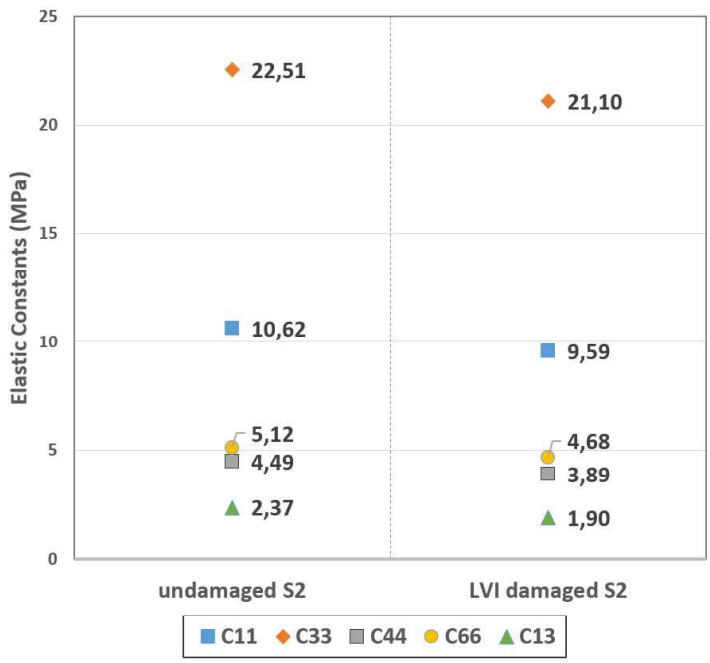

Figure 15 Elastic constants of the undamaged and LVI damaged sample S2

Here we notice a greater reduction of the elastic constants due to the LVI damage compared to what happen for the QSI damage. In particular, we have:

- a reduction of about 9% to 13% of the elastic constants C_{11} (extensional stiffness in the direction of x_1-axis, i.e. the direction of the impact), C_{44} and C_{66} (shear stiffness components related to the propagation plane π_{12});
- a reduction of about 6% of the elastic constant C_{33} (extensional stiffness in the direction of x_3-axis, i.e. the transverse isotropy axis);
- a reduction of about 10% of the shear elastic constant C_{13}.

4.3. Anisotropic damage tensor components

For a more consistent *quantitative* evaluation of the damage, the six non-trivial components of the fourth order damage tensor **D** have been determined by (11)-(12), starting from the elastic constants of the undamaged and of the damaged materials, both for the QSI damaged sample S1 and the LVI damaged sample S2. For convenience, we compare in Fig. 16 the value of the components of the damage tensor **D** obtained for the QSI damaged and for the LVI damaged composite.

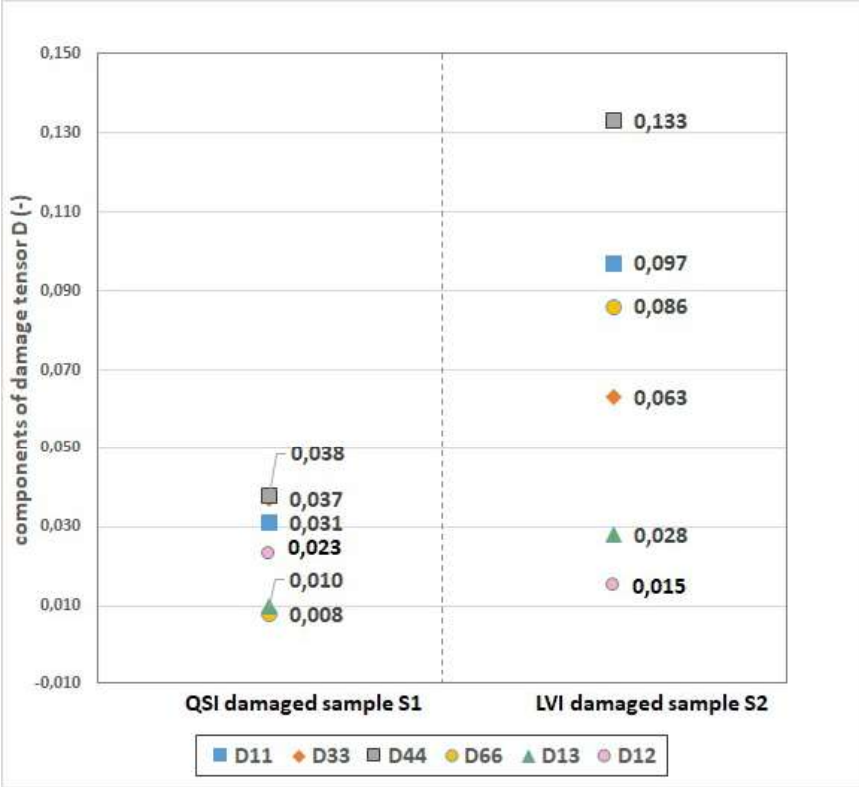

Figure 16 Components of the damage tensor for the QSI damaged and LVI damaged samples.

First, we notice that the norm of the damage tensor **D** is equal to 0.007 for the QSI damaged sample S1 and to 0.024 for the LVI damaged sample S2: this overall measure shows that the damage induced by the dynamic LVI test is much more than the damage induced by the ideally equivalent QSI test (3.5 times greater in terms of |**D**|).

In detail, the comparison of the corresponding components of **D** evaluated for the QSI damaged sample and for the LVI damaged sample allows us for some further considerations about the differences between the damage effects involved in the two different damage tests performed.

For the QSI damaged sample we have that the component D_{11}=0.031, related to the extensional behavior in the direction of the impact x_1, is very close to the component D_{33}=0.037, related to the extensional behavior in the direction of the fibers x_3 (transverse isotropy axis), and to the component D_{44}=0.038, related to the shear behavior in the planes π_{12} and π_{23} (the latter is orthogonal to the direction of the impact). This shows a quite homogeneous additional anisotropy effect due to the QSI damage. The remaining components of **D** are very small, denoting scarce damage effects.

On the contrary, for the LVI damaged composite we do not observe an homogeneous additional anisotropy effect, since there are larger differences between the components of **D**. In particular, the components D_{11}=0.097, D_{33}=0.063 and D_{44}=0.133 denote a significant change of the elastic behavior due to the LVI damage, markedly different for what concerns the extensional behavior in the

directions of the impact x_1 and of the fibers x_3, and the shear behavior in the planes π_{12} and π_{23}, the latter orthogonal to the impact direction. Moreover, the component D_{66}=0.086 is much greater than the corresponding component evaluated for QSI damage (D_{66}=0.008): this indicates that also the shear behavior in the plane π_{13} has been appreciably modified by the LVI damage. The remaining components of **D** are quite smaller.

Finally, although our model is purely macroscopic, we can try to give a physical interpretation to the fact that the value of the component D_{33} (related to the extensional behavior in the direction of the fibers) turns out to be smaller than to value of the component D_{11} (related to the extensional behavior in the direction of the impact). Indeed, it is possible to assume that the LVI impact test has not involved fiber fractures, and that the damage consists essentially in a fiber-matrix debonding or in matrix microcraks.

5. Conclusions

Here, by studying of the variation of the acoustic response in goniometric ultrasonic immersion tests, we have analyzed the damage induced in GFRP composite laminates by LVI and QSI damage tests. The latter have been performed with a small impact energy, in order to simulate some sneaky impact damage scenario possible during the service life of structural components, in particular for the case of composite wind turbine blades. To this aim, the damage is related to the damage induced anisotropy superimposed on the constitutive anisotropy of the composite. According to the literature, the performed LVI and QSI damage tests have been arranged such that an similar level of damage has to be expected in both cases.

Our results show that by the proposed experimental approach is very effective, since it is possible to quantitatively characterize damages even of small entity in GFRP composite laminates. Moreover, the damage model employed, strictly related to the experimental results, allows for a quantitative macroscopic comparison of damage of different kinds.

For composites, depending on the features of the damage, a variation of the acoustic axes and/or a variation of the shape of the slowness surfaces may occur. Anyway here, after both the performed damage tests, QSI and LVI, since the hemispherical impactor has acted in a principal direction of anisotropy (x_1-direction) the observed damage do not modifies the class of material symmetry of the composite, which remains transversely isotropic.

Beside the observed similarities, some differences between LVI and QSI damage have been determined. Indeed, we notice for the QSI damaged composite a slight and uniform variation of the

slowness curves for each kind of ultrasonic waves, and this correspond to the fact that QSI test has induced only a small damage anisotropy. Instead, for the LVI damaged composite we observe a more marked increment of the values of slowness for quasi-longitudinal waves, especially near the direction of the x1-axis (direction of the impact). Moreover, the slowness of quasi-shear waves for the undamaged and the damaged composite are similar near the x1-axis, but differs near the x3-axis, where we notice a readable increment of the slowness for the damaged composite.

For a quantitative evaluation of the difference between the damage induced in LVI tests and QSI tests, we have determined the components of the damage tensor **D**. According to what we presented in Sect. 4.3, the differences between LVI damage and QSI damage are evident: this pushes to further deepen the topic of the equivalence between LVI tests and QSI tests for GFRP composites, expecially for the case of low energy impacts.

The values assumed by the components of the damage tensor D might be related to some micromechanical features of the damage (fiber fracture, matrix fracture, fiber-matrix debondig, etc.). To this aim, it would be necessary to make suitable micromechanical experimental observations, to be compared with the ultrasonically characterized damage measure. Moreover, further improvements of the proposed approach may be obtained by combining experimental tests with suitable advanced numerical simulations of the phenomena involved in ultrasonic experiments on damaged, delaminated and cracked composites, like those proposed in [51].

We underline that the capability of ultrasonic goniometric tests of giving a broad description of the variation of the acoustic response of the material, and the features of the adopted damage model can be exploited for the characterization of more complex damage scenarios, like those due to impacts in directions oblique to the principal axes of anisotropy. Of course, those scenarios are experimentally inaccessible for the conventional LVI and QSI tests. Furthermore, the same approach can be also used for new complex materials, that are experiencing a growing interest and a fast diffusion in the various areas of engineering applications [52,53].

Finally, we notice that the effectiveness of the proposed approach is also related to the possibility of using other ultrasonic techniques, e.g., laser-ultrasonic techniques, and to the possibility of incorporating ultrasonic scanner in suitable devices for in-situ inspection of the structural components in service conditions.

References

[1] Castellano A, Foti P, Fraddosio A, Marzano S, Piccioni MD. The ultrasonic C-Scan

technique for damage evaluation of GFRP composite materials. Int J Mech 2016;10:206–12.

[2] Spronk SWF, Kersemans M, De Baerdemaeker JCA, Gilabert FA, Sevenois RDB, Garoz D, et al. Comparing damage from low-velocity impact and quasi-static indentation in automotive carbon/epoxy and glass/polyamide-6 laminates. Polym Test 2018;65:231–41. doi:10.1016/j.polymertesting.2017.11.023.

[3] Yahaya R, Sapuan SM, Jawaid M, Leman Z, Zainudin ES. Quasi-static penetration and ballistic properties of kenaf-aramid hybrid composites. Mater Des 2014;63:775–82. doi:10.1016/j.matdes.2014.07.010.

[4] Sutherland LS, Guedes Soares C. The use of quasi-static testing to obtain the low-velocity impact damage resistance of marine GRP laminates. Compos Part B Eng 2012;43:1459–67. doi:10.1016/j.compositesb.2012.01.002.

[5] Quadrino A, Penna R, Feo L, Nisticò N. Mechanical characterization of pultruded elements: Fiber orientation influence vs web-flange junction local problem. Experimental and numerical tests. Compos Part B Eng 2018;142:68–84. doi:10.1016/j.compositesb.2018.01.001.

[6] Castellano A, Foti P, Fraddosio A, Marzano S, Mininno G, Piccioni MD. Seismic Response of a Historic Masonry Construction Isolated by Stable Unbonded Fiber-Reinforced Elastomeric Isolators (SU-FREI). Key Eng Mater 2014;628:160–7. doi:10.4028/www.scientific.net/KEM.628.160.

[7] Gliszczynski A. Numerical and experimental investigations of the low velocity impact in GFRP plates. Compos Part B Eng 2018;138:181–93. doi:10.1016/j.compositesb.2017.11.039.

[8] Yudhanto A, Wafai H, Lubineau G, Yaldiz R, Verghese N. Characterizing the influence of matrix ductility on damage phenomenology in continuous fiber-reinforced thermoplastic laminates undergoing quasi-static indentation. Compos Struct 2018;186:324–34. doi:10.1016/j.compstruct.2017.12.028.

[9] Aoki Y, Suemasu H, Ishikawa T. Damage propagation in CFRP laminates subjected to low velocity impact and static indentation. Adv Compos Mater Off J Japan Soc Compos Mater 2007;16:45–61. doi:10.1163/156855107779755318.

[10] Gemi L, Sinan Şahin Ö, Akdemir A. Experimental investigation of fatigue damage formation of hybrid pipes subjected to impact loading under internal pre-stress. Compos Part B Eng 2017;119:196–205. doi:10.1016/j.compositesb.2017.03.051.

[11] Gemi L, Kara M, Avci A. Low velocity impact response of prestressed functionally graded hybrid pipes. Compos Part B Eng 2016;106:154–63. doi:10.1016/j.compositesb.2016.09.025.

[12] Lee SM, Zahuta P. Instrumented Impact and Static Indentation of Composites. J Compos

Mater 1991;25:204–22. doi:10.1177/002199839102500205.

[13] Azwan SMS, Yazid YM, Amran A, Abdi B. Quasi-Static Indentation Behaviour of Glass Fibre Reinforced Polymer. Adv Mater Res 2014;970:317–9. doi:10.4028/www.scientific.net/AMR.970.317.

[14] Kaczmarek H, Maison S. Comparative ultrasonic analysis of damage in CFRP under static indentation and low-velocity impact. Compos Sci Technol 1994;51:11–26. doi:10.1016/0266-3538(94)90152-X.

[15] Bull DJ, Spearing SM, Sinclair I. Investigation of the response to low velocity impact and quasi-static indentation loading of particle-toughened carbon-fibre composite materials. Compos Part A Appl Sci Manuf 2015;74:38–46. doi:10.1016/j.compositesa.2015.03.016.

[16] De Luca A, Caputo F, Sharif Khodaei Z, Aliabadi MH. Damage characterization of composite plates under low velocity impact using ultrasonic guided waves. Compos Part B Eng 2018;138:168–80. doi:10.1016/j.compositesb.2017.11.042.

[17] Palumbo D, Galietti U. Damage Investigation in Composite Materials by Means of New Thermal Data Processing Procedures. Strain, vol. 52, 2016, p. 276–85. doi:10.1111/str.12179.

[18] Palumbo D, De Finis R, Demelio PG, Galietti U. A new rapid thermographic method to assess the fatigue limit in GFRP composites. Compos Part B Eng 2016;103:60–7. doi:10.1016/j.compositesb.2016.08.007.

[19] Pagliarulo V, Rocco A, Langella A, Riccio A, Ferraro P, Antonucci V, et al. Impact damage investigation on composite laminates: Comparison among different NDT methods and numerical simulation. Meas Sci Technol 2015;26. doi:10.1088/0957-0233/26/8/085603.

[20] Baste S, Aristégui C. Induced anisotropy and crack systems orientations of a ceramic matrix composite under off-principal axis loading. Mech Mater 1998;29:19–41. doi:10.1016/S0167-6636(98)00003-9.

[21] Marguères P, Meraghni F. Damage induced anisotropy and stiffness reduction evaluation in composite materials using ultrasonic wave transmission. Compos Part A Appl Sci Manuf 2013;45:134–44. doi:10.1016/j.compositesa.2012.09.007.

[22] Margueres P, Meraghni F, Benzeggagh ML. Comparison of stiffness measurements and damage investigation techniques for a fatigued and post-impact fatigued GFRP composite obtained by RTM process. Compos Part A Appl Sci Manuf 2000;31:151–63. doi:10.1016/S1359-835X(99)00061-5.

[23] Siva Shashidhara Reddy S, Balasubramaniam K, Krishnamurthy C V., Shankar M. Ultrasonic goniometry immersion techniques for the measurement of elastic moduli. Compos

Struct 2005;67:3–17. doi:10.1016/j.compstruct.2004.01.008.

[24] Castellano A, Foti P, Fraddosio A, Marzano S, Piccioni MD. Ultrasonic immersion tests for mechanical characterization of multilayered anisotropic materials. EESMS 2014 - 2014 IEEE Work. Environ. Energy Struct. Monit. Syst. Proc., 2014, p. 63–8. doi:10.1109/EESMS.2014.6923266.

[25] Castellano A, Foti P, Fraddosio A, Marzano S, Piccioni MD. Mechanical characterization of CFRP composites by ultrasonic immersion tests: Experimental and numerical approaches. Compos Part B Eng 2014;66:299–310. doi:10.1016/j.compositesb.2014.04.024.

[26] Baste S, Audoin B. On internal variables in anisotropic damage. Eur J Mech A/Solids 1991;10:587–606.

[27] Baste S, Audoin B. Ultrasonic evaluation of stiffness tensor changes and associated anisotropic damage in a ceramics matrix composite. J Appl Mech 1994;61:309–16.

[28] Castellano A, Fraddosio A, Marzano S, Daniele Piccioni M. Some advancements in the ultrasonic evaluation of initial stress states by the analysis of the acoustoelastic effect. Procedia Eng., vol. 199, 2017. doi:10.1016/j.proeng.2017.09.494.

[29] Castellano A, Foti P, Fraddosio A, Marzano S, Paparella F, Piccioni MD. Monitoring applied and residual stress in materials and structures by non-destructive acoustoelastic techniques. EESMS 2016 - 2016 IEEE Work. Environ. Energy, Struct. Monit. Syst. Proc., 2016. doi:10.1109/EESMS.2016.7504830.

[30] Gurtin ME. The Linear Theory of Elasticity. Linear Theor. Elast. Thermoelast., 1973, p. 1–295. doi:10.1007/978-3-662-39776-3_1.

[31] Castellano A, Fraddosio A, Piccioni MD. Ultrasonic goniometric immersion tests for the characterization of fatigue post-LVI damage induced anisotropy superimposed to the constitutive anisotropy of polymer composites. Compos Part B Eng 2017;116:122–36. doi:10.1016/j.compositesb.2017.02.025.

[32] Royer D, Dieulesaint E. Elastic Waves in Solids: Free and guided propagation. vol. 1. 2000.

[33] Payton RG. Wave Propagation in Transversely Isotropic Media. 1983.

[34] Krajcinovic DK. Continuum damage mechanics. Appl Mech Rev 1984;37:1–6.

[35] Lemaitre J. A course on damage mechanics. Springer. 1992.

[36] Murakami S. Anisotropic aspects of material damage and application of continuum damage mechanics. Kraj. D, Lemaitre J Contin. Damage Mech. Theory Appl., 1987, p. 91–133.

[37] Kestin J, Rice JR. Paradoxes in the Application of Thermodynamics to Strained Solids. A Crit. Rev. Thermodyn., 1970, p. 275–98.

[38] Germain P. LA METHODE DES PUISSANCES VIRTUELLES EN MECANIQUE DES

MILIEUX CONTINUS - 1. THEORIE DU SECOND GRADIENT. J Mec Theor Appl 1973;12:235–74.

[39] Kachanov LM. Time of the rupture process under creep conditions. Izv Akad Nauk S S R Otd Tech Nauk 1958;8:26–31. doi:citeulike-article-id:5466815.

[40] Rabotnov Yu N. Creep rupture. Hetenyi M, Vincenti M Proc. Appl. Mech. Conf. Stanford U, Berlin: 1968.

[41] Chaboche JL. Sur l'utilisation des variables d'etat interne pour la description du comportement viscoplastique et de la rupture par endommagement. Nowacki WK Problèmes Non-Linéaires Mécanique (Proceedings French-Polish Symp. Cracow 1977). PWN (State Publ. House Sci. Warsaw, 1980, p. 137–59.

[42] Lemaitre J, Chaboche J-L. Aspect phénoménologique de la rupture par endommagement. J Mécanique Appliquée 1978;2:317–365.

[43] Cordebois JP; Sidoroff F. Endommagement anisotrope en élasticité et plasticité. J Mécanique Théorique Appliquée Numéro Spécial 1982:45–60.

[44] Semenov AS. Symmetrization of the effective stress tensor for anisotropic damaged continua. St Petersbg Polytech Univ J Phys Math 2017;3:271–83. doi:https://doi.org/10.1016/j.spjpm.2017.09.005.

[45] Fosdick R, Foti P, Fraddosio A, Marzano S, Piccioni MD. A lower bound estimate of the critical load in bifurcation analysis for incompressible elastic solids. Math Mech Solids 2015;20:53–79. doi:10.1177/1081286514543599.

[46] Cauvin A; Testa R. Damage mechanics: basic variables in continuum theories. Int J Solids Struct 1999;36:747–61.

[47] Olsen-Kettle L. Using ultrasonic investigations to develop anisotropic damage models for initially transverse isotropic materials undergoing damage to remain transverse isotropic. Int J Solids Struct 2018. doi:10.1016/j.ijsolstr.2018.01.007.

[48] ASTM D6264. Standard Test Method for Measuring the Damage Resistance of a Fiber-Reinforced Polymer-Matrix Composite to a Concentrated Quasi-Static Indentation Force 2017.

[49] Subcommittee D30.05 on Structural Test Methods. ASTM D7136 / D7136M-15, Standard Test Method for Measuring the Damage Resistance of a Fiber-Reinforced Polymer Matrix Composite to a Drop-Weight Impact Event. ASTM B. Stand. Vol. 15.03, 2015. doi:10.1520/D7136_D7136M-15.

[50] Castagnède B, Jenkins JT, Sachse W, Baste S. Optimal determination of the elastic constants of composite materials from ultrasonic wave-speed measurements. J Appl Phys

1990;67:2753–61. doi:10.1063/1.345441.

[51] Hafezi MH, Alebrahim R, Kundu T. Peri-ultrasound for modeling linear and nonlinear ultrasonic response. Ultrasonics 2017;80:47–57. doi:10.1016/j.ultras.2017.04.015.

[52] Barretta R, Feo L, Luciano R. Some closed-form solutions of functionally graded beams undergoing nonuniform torsion. Compos Struct 2015;123:132–6. doi:10.1016/j.compstruct.2014.12.027.

[53] Mancusi G, Fabbrocino F, Feo L, Fraternali F. Size effect and dynamic properties of 2D lattice materials. Compos Part B Eng 2017;112. doi:10.1016/j.compositesb.2016.12.026.